January 27, 2017

Dr Marie-Claire ten Veldhuis
Editor
Hydrology and Earth System Sciences (HESS)

RE: hess-2016-530

Dear Editor,

Please find enclosed the revised manuscript: "Partitioning the impacts of spatial and climatological rainfall variability in urban drainage modelling", previously entitled "Partitioning spatial and temporal rainfall variability in urban drainage modelling" by Nadav Peleg, Frank Blumensaat, Peter Molnar, Simone Fatichi and Paolo Burlando. The manuscript has been revised according to the comments of the two reviewers. We would like to thank the Editor and the two reviewers (Susana Ochoa Rodriguez and an anonymous reviewer) for their efforts and constructive comments. Detailed answers to the reviewers' comments are given below.

Reviewer #1:

General Comments: The paper is very interesting and tries to add new knowledge to the field of urban hydrology. The use of stochastic rainfall generators and their impact in urban drainage is very important and recent. The authors try to quantify, not only the impact of spatial component of rainfall, but also its temporal component.
We thank the reviewer for his time and effort reviewing our manuscript.
Specific comments:

1) It would be interesting to know the drainage area of each location where the flow analysis was conducted.
Contributing area: 11.5 ha total area (5.3 ha impervious area) is connected to location A and 30.2 ha (13.6 ha) is connected to locations B and C, whereas the two latter locations are constrained through the overflow weir structure. This information was added in manuscript.

2) Why you didn't test more locations in the upstream part of the catchment. It would be interesting to see the climate and spatial contribution in smaller drainage areas (for example an upstream pipe and one not affected by hydraulic structures, such as CSOs.) This would be important, since some authors showed that upstream pipes are more sensitive to spatial variability (eg. Gires et al., 2012)
Location A is located upstream of the CSO, but clearly not affected by water backing up due to the hydraulic constraint at the CSO structure. Examining the effects of contributing area on peak flows depending on the topological location within the network indeed requires analyzing further locations, and it is an interesting point to examine. However, we did not include this aspect into our analysis for two reasons: (i) we did not want to repeat analyses that had been done already in previous studies (e.g. by Gires et al., 2012); and (ii) the examined system is too small to obtain a representative answer on this aspect. Instead, we focus on the system response for three distinctively chosen, characteristic locations, differing regarding their functional hierarchy (A - upstream in the catchment, B – downstream of overflow structure at the overflow outlet, C – downstream overflow structure in the carry-on flow). By doing so, we believe that the analysis has an added value since effects of spatial and climatological rainfall variability can be differentiated depending on the *function* of the network element.
We still think it would be interesting to see if results shown by Gires et al. (2012) on the spatial variability in the upper part of the catchment, similar like location A, can be reproduced. However, we clearly think a larger urban drainage network, i.e. a larger number of nodes, should be examined following the same methodology to come to a representative conclusion with this regard. Finally, we addressed this issue in the revised version of the manuscript by discussing potential options to conduct this extended analysis depending on the topological location in the network:

"The three locations analyzed in this study were deliberately chosen according to their functional hierarchy within the combined drainage system (i.e. inner network node, carry-on flow and overflow). By doing so, we can clearly differentiate the effect of spatial and climatological rainfall variability on elements depending on their function within the network. On the other hand, previous studies showed a tendency that conduits located upstream, not affected by hydraulically constraining structures, are more sensitive to rainfall spatial variability in comparison to conduits located downstream (e.g. Gires et al., 2012). While it would be interesting to further investigate flow variability due to different spatial rainfall characteristics (e.g. the rainfall spatial correlation) at various upstream locations (similar as location A), this type of analysis would require larger drainage networks in comparison to the one presented here. Future studies will benefit from examining several different urban drainage systems with rainfall input from different high-resolution products to test the robustness of the findings".

3) Is there flooding in any node? How did your SWMM model deal with it? If there is flooding, what is the impact in the flow return period.

Yes, flooding occurs at several nodes when simulating the 30 year period(s). For example at location A, for the reference period 1980 – 2010 surface flooding was estimated for 34 events (0.1 – 1.5 hours of duration) using measured single gauge rainfall data. The number of nodes at which flooding is observed is limited; location A is one of the few locations (8 – 10 in total) where flooding occurs. Surface flooding is accounted for by allowing excess water to leave a manhole in case sewer capacity is exceeded. Due to the lack of detailed land use and surface topography data it was found inadequate to define a node-specific 'ponding area' (i.e. surface area that is available allowing the water to spread at the surface around a manhole). Hence surface flooding is taken into account but excess water leaving the manhole is routed into a virtual sink and does not re-enter through the manhole lid after sewer capacity is available again. We evaluated simulation runs with different simulation options to consider flooded water volume re-entering the system (namely: a) ponding area left undefined; b) definition of generally 100 m² 'ponding area') specifically focusing on deviations of flow rates at study relevant locations. Results from benchmarking simulations (see collection of figures below; notated with *F#*) clearly show that choosing different simulation options does not significantly affect the in-sewer flow rates, which had been selected as evaluation criterion in this study. We verified this for short periods, i.e. a series of events (example in F1 to F3, upper graphs), as well as for long terms (example in F1 to F3, lower graphs), whereas series labelled as '*ref data*' stand for simulations without having a ponding area defined and series labelled with '*sim data*' represent simulation for which a ponding area of 100m² had been defined. Performance metrics (Bias, Nash-Sutcliff-Efficiency, Index of Agreement, volume balance) indicate the low order of magnitude for flow rate, i.e. flow return period deviations. Still, for simulations for which excess water is not allowed to re-enter the system ('*ref data*', '*Vref*') the flow volume is – as expected - slightly lower. The following paragraph was added to the manuscript in Section 3.4 explain how surface flooding is considered in the study: "Surface flooding is accounted for by allowing excess water to leave a manhole in case sewer capacity is exceeded. Due to the lack of detailed land use and surface topography data at meter scale it was found inadequate to further define a manhole-specific "ponding area" allowing the water to spread at the surface around a manhole. Hence excess water leaving the manhole is routed into a virtual sink and does not re-enter the system even though sewer capacity is available again.".

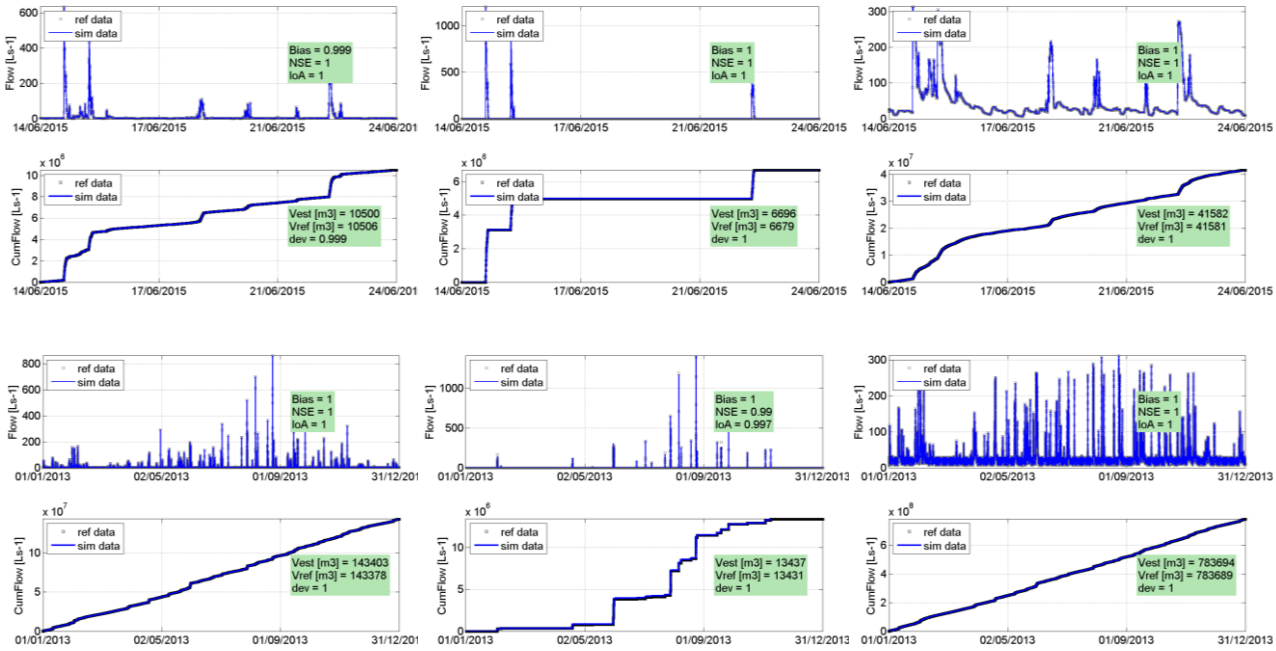

F1: Location A F2: Location B F3: Location C

4) Figure 3 could be improved showing the inverse-CDF curve of all the 30 events, not only the mean.
It is represented (shaded red area) for the 5-95 quantile of all 30 events. The range is very thin and almost unnoticeable.

5) In section 3 (1st paragraph) is not clear why do you use IDF and FDF curves, instead of the obtained/simulated values. I agree with the strategy, but a clear explanation should be added.
A sentence rationalizing the use of a parametric distribution fitting to compute the IDF and FDF curves was added to Section 3.5: "The fitting of the parametric distribution is a required step for the partition analysis to be conducted (see next section) as it results in a continuous estimates of the curves quantiles (i.e. the return period)".

6) Figure 2 needs a better explanation
The caption of Figure 2 was changed as follows: "A schematic illustration of the methods used in this study: (i) STREAP model was used to simulate multiple realizations of 2-D rain fields based on radar and gauged data (Section 3.2); (ii) rainfall was generated for four distinct cases which were defined in order to explicitly account for the climate variability, spatial rainfall variability and total variability of the flow (3.3); (iii) EPA SWMM model was used to calculate the flow over the catchment (3.4); (iv) IDF and FDF curves were computed for the annual maxima of the mean areal rainfall and flow, respectively, at three different locations (3.5); and (v) the total flow variability was partitioned (3.6)".

Technical corrections:
1) Figure 2 needs more quality
The quality of Figure 2 was enhanced to 600 dpi.

2) In Figure 5 legend, where is "quantile range is than calculated for each" should be "quantile range is then calculated for each"
Thank you for pointing out this typo. The sentence was corrected.

Reviewer #2 (Susana Ochoa Rodriguez):

This study explores the influence of the spatial and natural climatological variability of rainfall on rainfall and associated flow return period estimation in urban areas. For this purpose, a stochastic rainfall generator was employed to generate rainfall time series with and without spatial variability. The resulting rainfall time series (corresponding to 4 different scenarios including combinations of spatial and climatological rainfall variability) were applied as input to the urban drainage model of a test catchment in Lucerne, Switzerland. Based on the results, both rainfall and flow return periods were computed and the individual influence of spatial and climatological rainfall variability on extremes was quantified. The study is very interesting and the results constitute a valuable contribution towards improved design of urban drainage systems. The paper is well written and we certainly enjoyed reading it.
We thank the reviewers for their kind words and for the time and effort reviewing our manuscript.

I suggest that the authors clarify/address the following points prior to publication:

1. Please specify the drainage area of the points at which urban flows were analysed. As highlighted in previous studies, the drainage area of interest has a significant impact on the impact of spatial rainfall variability on simulated urban flows. In fact, in the figures provided in the supplement of the manuscript under consideration, it can be seen that the impact of spatial variability is somewhat different at the different locations at which flows are analysed. This is likely partly due to differences in the drainage areas associated to each point under consideration (this is, the areas upstream of the point of interest). Please provide information about the drainage areas under consideration and briefly analyse the impact of this factor on your results (a detailed analysis of this could also be suggested as 'future work').
The drainage area connected to locations of interest is: 11.5 ha total area (5.3 ha impervious area) are connected to location A and 30.2 ha (13.6 ha) are connected to locations B and C, whereas locations B and C are constrained through the overflow weir structure. This information was added in the manuscript. Location A is located upstream of the CSO and is not affected by it. In the study we focus on the system response for three distinctively chosen, characteristic locations, differing regarding their functional hierarchy (A - upstream in the catchment, B – downstream of overflow structure at the overflow outlet, C – downstream overflow structure in the carry-on flow). By doing so, we can show that effects due spatial and climatological rainfall variability need to be differentiated depending on the *function* of the corresponding network element and not only depending on the contributing area. Examining the effects of contributing area on peak flows depending on the topological location within the network indeed requires analyzing further locations within the drainage system upstream of the hydraulically constraining structures. Although this analysis is interesting, it was not a key aspect of this paper. We think it will require a larger drainage network than examined in the presented case study. We addressed this issue in the discussion section in the revised version of the manuscript as follows:
"The three locations analyzed in this study were deliberately chosen according to their functional hierarchy within the combined drainage system (i.e. inner network node, carry-on flow and overflow). By doing so, we can clearly differentiate the effect of spatial and climatological rainfall variability on elements depending on their function within the network. On the other hand, previous studies showed a tendency that conduits located upstream, not affected by hydraulically constraining structures, are more sensitive to rainfall spatial variability in comparison to conduits located downstream (e.g. Gires et al., 2012). While it would be interesting to further investigate flow variability due to different spatial rainfall characteristics (e.g. the rainfall spatial correlation) at various upstream locations (similar as location A), this type of analysis would require larger drainage networks in comparison to the one presented here. Future studies will benefit from examining several different urban drainage systems with rainfall input from different high-resolution products to test the robustness of the findings".

2. While 2 km radar data were employed to calibrate the rainfall generator, 100 m spatial data were then generated. Please discuss the implications of this and whether the downscaling model that was employed accounts for scaling, thus making it appropriate to downscale down to 100 m (although the model was only calibrated based on 2km data).

The rainfall model was downscaled to 100 m resolution using power laws functions, as mentioned in Section 3.2.1. A figure was added in the supplementary material (new Figure S1) showing the scaling of the rainfall coefficient of variation from the weather radar resolution to the high-resolution required for the analysis:

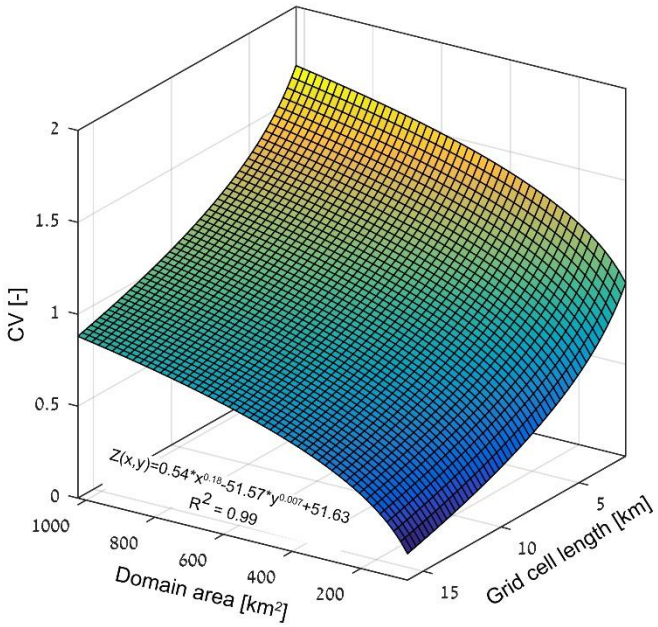

with the following caption: "**Figure S1.** Rainfall coefficient of variation (CV) power law surface-fit for temporal resolution of 5 min. X-axis refer to the domain area, Y-axis refer to the dimension of the rainfall grid cell and Z-axis represent the rainfall CV. Data was derived from MeteoSwiss weather radar system for domain areas of 64-1024 km^2 and grid sizes of 2-16 km for domains overlapping the studied catchment. For the case study, rainfall was generated over an area of 2.25 km^2 using grid size of 100 m, thus a CV of 1.5 was used".

A short explanation was added to the text for the choice of rainfall spatial correlation structure used: "In addition, no direct measurements are available to estimate the small-scale rainfall spatial correlation structure for this region. The spatial structure was estimated using data from three dense rain-gauge networks (Moszkowicz, 2000; Müller and Haberlandt, 2016; Peleg et al., 2013), recording rainfall over small spatial distances (i.e. in the scale of 10^1–10^2 m) and temporal scales (i.e. 5–10 min)". A new figure (Fig. S2) was added to the supplementary material:

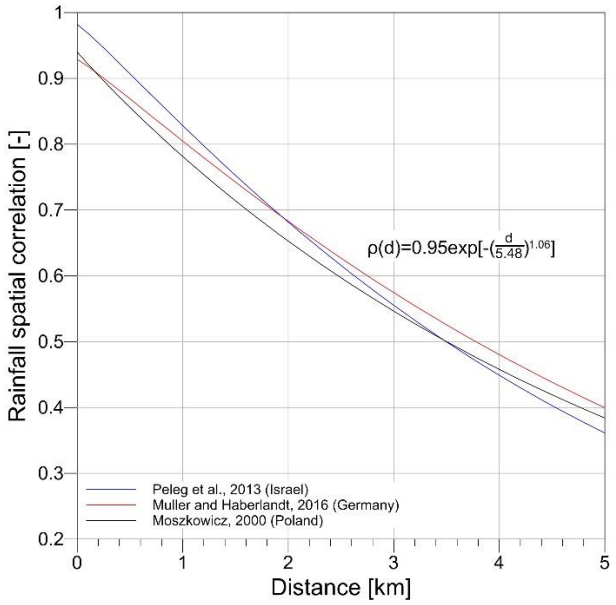

with the following caption: "**Figure S2.** Small-scale spatial correlation structure for 5-min temporal resolution as was recorded using dense rain-gauge networks in Germany, Poland and Israel. The average correlation structure of the three (expressed by the three-parameter exponential function given in the figure) was used in this study".

3. The temporal resolution adopted in the study (10 min) may be too coarse for urban applications and may result in smoothing of urban flows, which may in turn result in underestimation of flow extremes (as indicated in Ochoa-Rodriguez et al. (2015), temporal resolutions <= 5 min are required for urban hydrological applications, with resolutions of 10 min leading to large underestimation of peak flows. Likewise, Wang et al. (2015) showed results of flow simulations resulting from rainfall inputs at temporal resolutions from 1 to 10 minutes and compared them against flow observations; the results associated to 10 min rainfall inputs largely underestimated observed flow peaks and resulted in 'distorted' hydrographs). I understand that the temporal resolution of choice was likely constrained by the resolution at which rain gauge rainfall records were available. Please discuss the implications and limitations of the temporal resolution of choice and clearly mention in the future work section that tests should be conducted at finer temporal resolutions.

The rainfall temporal resolution was indeed set to 10 min following the temporal resolution of observed rainfall records. We do agree that temporal resolution of rainfall data used as model input significantly influences flow dynamics including peak flows. We added the following sentence in the manuscript in section 3.2: "For this analysis, rainfall was generated with a spatial resolution of 100 m x 100 m for a domain size of 1.5 km x 1.5 km (see mesh in Fig. 1) and a temporal resolution of 10 min. *For urban drainage applications 10 min can be considered a rather coarse temporal discretization, however we searched consistency with the observed rainfall record which is only available in 10 min resolution.*".

We are fully aware of that this is a suboptimal compromise. However, considering the fact that we calibrated the model using a one-year measured flow reference record and calibration results clearly show that the model can reproduce flow dynamics adequately, we think that using a 10 min rainfall resolution is more justified than generating rainfall data with a higher temporal resolution than the observed rainfall reference.

4. The current title of the paper is rather misleading and I would suggest changing it to better reflect the purpose and focus of the study. For example, the focus on extreme values / return period should somehow be mentioned. Furthermore, I would suggest changing 'temporal variability' to 'natural climatological variability'. The term temporal variability conveys the idea of temporal resolution, which, as described above, is not the purpose of this study and is in fact one of its shortcomings.

We agree with the reviewer comment. A new title for the manuscript is suggested: "Partitioning the impacts of spatial and climatological rainfall variability in urban drainage modelling".

Finally, we would like again to express our thanks to the Editor and to the two reviewers who have helped us to significantly improve the paper.

Sincerely,

Nadav Peleg and Frank Blumensaat on behalf of the authorship

Partitioning the impacts of spatial and ~~temporal~~ climatological rainfall variability in urban drainage modelling

Nadav Peleg[1], Frank Blumensaat[2,3], Peter Molnar[1], Simone Fatichi[1], and Paolo Burlando[1]

[1]ETH Zurich, Institute of Environmental Engineering, Hydrology and Water Resources Management, Zurich, Switzerland
[2]Swiss Federal Institute of Aquatic Science and Technology, Eawag, Dübendorf, Switzerland
[3]ETH Zurich, Institute of Environmental Engineering, Urban Water Systems, Zurich, Switzerland

Correspondence to: Nadav Peleg (nadav.peleg@sccer-soe.ethz.ch)

Abstract. The performance of urban drainage systems is typically examined using hydrological and hydrodynamic models where rainfall input is uniformly distributed~~and derived from a single rain–gauge or spatially distributed and obtained from a weather radar system~~, i.e. derived from one single or very few rain–gauges. When models are fed with a single rainfall realization, the response of the urban drainage system to the spatio-temporal variability of rainfall remains unexplored. High resolution stochastic rainfall generators allow studying the response and sensitivity of urban drainage networks to these spatial and temporal rainfall variabilities. The goal in this study was to understand how climate variability and spatial rainfall variability, jointly or individually considered, affect the response of a calibrated hydrodynamic urban drainage model. A stochastic high resolution rainfall generator (STREAP) was used to simulate many realizations of rainfall for a period of 30 years, accounting for both climate variability and spatial rainfall variability. The generated rainfall was then used as input into a calibrated hydrodynamic model (EPA SWMM) ~~to simulate~~ for simulating surface runoff and channel flow ~~for~~ in a small urban catchment in the city of Lucerne, Switzerland. The variability of peak flows ~~at three different locations in the urban drainage network in~~ in response to rainfall of different return periods was evaluated at three different locations in the urban drainage network and partitioned among ~~it~~ its sources. We found that the main contribution to the total flow variability originates from the natural climate variability (on average over 74%). In addition, the contribution of spatial rainfall variability to the total flow variability was found to increase with longer return periods. This ~~implies~~ suggest that while the use of spatially distributed rainfall data can supply valuable information for sewer network design (typically based on rainfall with return periods from 5 to 15 years), there is a more pronounced relevance when conducting flood risk assessments for larger return periods. The results clearly show the importance of using stochastic rainfall generators in urban hydrology studies ~~not only to~~ to not only capture the total variability in the response of the urban drainage systems to heavy rainfall but also to ~~gain transparency regarding~~ identify the origin of this variability.

1 Introduction

Urban drainage systems are designed to ensure safe wastewater ~~handling~~ disposal (focus: dry weather) and adequate storm water ~~conveyance~~ handling (focus: wet weather). Whereas the variability of dry weather flows is rather low and well predictable, rain-induced flow dynamics ~~may cover~~ scale over several orders of magnitude and require stochastic analysis due

to the high variability of rainfall. The latter is often addressed by summarizing the rainfall input in the form of Intensity–Duration–Frequency (IDF) curves (e.g. Guo, 2006; Yazdanfar and Sharma, 2015), which are essentially relating maxima of rainfall intensity for a given duration to their return period (Koutsoyiannis et al., 1998). For urban drainage system design, engineers choose return periods for which they expect the urban drainage system to perform with a certain reliability (e.g. an acceptable number of failures such as overflows or flooding in a given return interval).

A common practice to evaluate the performance of urban drainage systems for different forcing situations is by using a model with a hydrological component to simulate the transformation of rainfall into runoff at the urban catchment scale and a hydrodynamic component to simulate the flow in the drainage system itself. Rainfall is defined as the most important input required by these models (Vaes et al., 2001). It is recommended to use high resolution rainfall data in space and time as an input because of the ~~fast~~ short concentration time of urban drainage systems, and because ~~this increases flow prediction accuracy and reduces~~ it reduces flow prediction uncertainty. The required spatial and temporal resolution depends on the size of the urban catchment, characteristics of the drainage system, and local climate. A general recommendation is to use rainfall data in a resolution similar to (or higher than) that produced by a typical X–band weather radar system, i.e. minutes in time and sub-kilometer in space (see discussion by Berne et al., 2004; Bruni et al., 2015; Ochoa-Rodriguez et al., 2015; Wright et al., 2014b).

Rainfall input may be given by observations of rain–gauges and weather radar~~, however this limits the analysis only~~ ; however this constrains the analysis to storms observed in a limited time period. Stochastic modeling of space-time rainfall fields on the other hand allows a full exploration of the potential impacts of space-time variability in rainfall on the urban drainage system. The *spatial rainfall variability* is defined as the variability derived from having multiple (stochastic) spatial rainfall distributions for a given rainfall. The temporal component, here referred to as *climate variability*, is defined as the variability derived from having multiple (natural) climate trajectories ~~forcing~~ generating different distribution of storms and rainfall intensities in time. It is also known as "internal variability" or "stochastic climate variability" (Deser et al., 2012; Fatichi et al., 2016; Hawkins and Sutton, 2009). The consideration is that observed rainfall represents only one trajectory of a given climate and producing stochastic rainfall based on observed rainfall statistics results in many ~~climate~~ realizations, each one equally probable (see for example Peleg et al., 2015).

The use of stochastic rainfall generators that account for both spatial rainfall distribution and temporal climatic variability in urban hydrology applications is still rather new. Wright et al. (2014a) used stochastic storm transposition to synthesize long records of rainfall based on radar rainfall fields over the metropolitan area of Charlotte, North Carolina (USA), in order to estimate the discharge return periods for points inside the urban catchment. McRobie et al. (2013) extended the earlier Willems method (Willems, 2001) to generate spatially distributed Gaussian rainfall cells based on weather radar data for the Counters Creek catchment sewerage system in London (UK). Simoes et al. (2015) produced stochastic urban pluvial flood hazard maps for the Cranbrook urban catchment (UK) using the McRobie et al. (2013) rainfall generator. Gires et al. (e.g., 2012, 2013) used a multifractal model to generate space-time rainfall fields for the same storm but with different spatial structures, to study their effect on the simulated flow in conduits in the Cranbrook catchment. The most recent stochastic rainfall generators that are

able to produce rainfall fields in a high spatial and temporal resolution and may be useful for urban applications are STREAP (Paschalis et al., 2013, 2014), HiReS-WG (Peleg and Morin, 2014) and STEPS (Foresti et al., 2016; Niemi et al., 2016).

The main objective of this paper is to investigate the relative contribution of the spatial versus climatic rainfall variability for flow peaks at different locations in the drainage network and for different return periods. We apply a new and advanced stochastic rainfall generator to simulate rainfall inputs for a small urban catchment in Lucerne (Switzerland) and simulate flow dynamics in the sewer system. The stochastic rainfall generator is used to simulate multiple ~~30–years~~ 30–year realizations of rainfall over the catchment, accounting for both climate variability and spatial rainfall variability. This work demonstrates the potential of high resolution stochastic rainfall generators for urban applications and the benefits gained compared to other methods, such as bootstrapping rainfall events from a long rainfall series.

2 Case Study

The case study is an urban catchment located near the city center of Lucerne, Switzerland (Fig. 1). The catchment in total covers 77.0 ha, whereas 30.2 ha are connected to the combined sewer network: 11.5 ha of total area (5.3 ha impervious area) are connected to location A and 30.2 ha (13.6 ha) are connected to locations B and C. The catchment drains towards Lake Lucerne, with higher gradients at the upper part and moderate to low gradients in the lower part. The drainage system consists of separate and combined sewers (storm water and foul sewage share one pipe infrastructure) with a total network length of 11.2 km; hereinafter only combined sewers are considered. Both storm water and wastewater flows are solely driven by gravity. An overflow structure is built in the lower part of the catchment to alleviate network capacity excess during heavy rainfall ~~.~~ (CSO location in Fig. 1). In this case, the carry-on flow towards the sewage treatment plant is hydraulically constrained (location B in Fig. 1), and excess water is spilled via a side-flow weir followed by a small retention tank (approximate 100 m^3) into Lake Lucerne (location C in Fig. 1).

The flow rate at the outlet of the combined sewer system (location B) is monitored for a period of ~~about~~ 12 months from July 2014 to June 2015. In order to reduce measurement uncertainty, the water level and flow velocity was recorded using two different combi-sensors with different monitoring techniques (in-situ Doppler-ultrasound technique, ex-situ ultrasound-radar technique) in parallel. The recording interval was set to 1 min and 15 min for the Doppler-ultrasound sensor and the ultrasound-radar sensor, respectively. ~~This data is used to calibrate and validate (split-sample approach) a hydrodynamic sewer model which was set up based on infrastructure data from the municipality cadaster database. More details on the catchment, particularly on the urban land use characteristics, the monitoring set-up, model calibration procedure are given in Tokarczyk et al. (2015) .~~

3 Methods and Data

A stochastic high resolution space-time rainfall generator was used to simulate multiple realizations of 2-D rain fields for 30 years. The rainfall was generated for four distinct cases which were defined in order to explicitly account for the climate

variability, spatial rainfall variability and total variability of the flow. The generated rainfall was used as an input into a hydrodynamic model. For each of the four cases, IDF curves were computed for the annual maxima of the mean areal rainfall and Flow–Duration–Frequency (FDF) curves were computed for annual flow maxima simulated at three different network elements, representing different aspects in the assessing of the performance of urban drainage systems. The total flow variability was partitioned into the part originating from climate variability and the ~~part~~ additional contribution due to spatial rainfall variability. The methods are illustrated in Fig. 2.

3.1 Rainfall Data

Rainfall data originate from two sources: a rain–gauge located about 2 km west to the test catchment (Fig. 1) and a C–band weather radar composite. Both devices are operated by MeteoSwiss, the Swiss Federal Office of Meteorology and Climatology.

The tipping bucket rain–gauge records rainfall in 10 min intervals with a precision of 0.1 mm. A 34 year record was used in this study, covering the period 1981–2014. High-resolution 10 min min data were benchmarked with hourly rainfall data (validated record provided by MeteoSwiss) and deviations were corrected. The length of the observed record allows an adequate estimation of the rainfall characteristics, especially regarding high rainfall intensities of short durations and with return periods up to 30 years. Climatological stationarity has been assumed for the observed record.

The high resolution radar rainfall data (2 km and 5 min) for the 8 year period 2003–2010 are from a third-generation weather radar system of MeteoSwiss (Gabella et al., 2005; Germann et al., 2006). Radar grid cells were examined for substantial ground clutter or beam blockage and errors were excluded. This data was only used for the study of the rainfall structure over the catchment and not for the calculation of IDF curves, as the accuracy of rainfall intensity recorded by the weather radar (binned data) is not ~~high enough~~ sufficient to address extremes. Extreme rainfall intensity for a 1 km spatial resolution can be analyzed in Switzerland (e.g. Panziera et al., 2016) using the fourth-generation weather radar system (Germann et al., 2015) or the gridded CombiPrecip products (Sideris et al., 2014). However, a longer period of high resolution rainfall from the latter mentioned products would be required in order to properly account for the climate variability discussed in this study.

3.2 Stochastic Rainfall Generator

Rainfall fields in a high spatial and temporal resolution were generated using the STREAP model (**S**pace-**T**ime **Re**alizations of **A**real **P**recipitation). STREAP was presented by Paschalis et al. (2013) and used to generate rainfall over a large rural catchment for flood investigations (Paschalis et al., 2014) and to analyze the variability of extreme rainfall intensity over radar-pixel scales (Peleg et al., 2016). It is composed of three hierarchical modules describing: (i) the storm arrival process; (ii) temporal evolution of the mean areal intensity and fraction of wet area during a storm; and (iii) evolution of the space–time structure of rainfall during a storm.

For this analysis, rainfall was generated with a spatial resolution of 100 m x 100 m for a domain size of 1.5 km x 1.5 km (see mesh in Fig. 1) and a temporal resolution of 10 min. For urban drainage applications 10 min can be considered a rather coarse temporal discretization, however we searched consistency with the observed rainfall record which is only available in 10 min resolution. The spatial resolution was chosen to roughly match the discretization required for the urban sub-catchments,

i.e. about two sub-catchments per ha resulting in 158 individual sub-catchments within 77 ha~~, and the temporal resolution was set to match the temporal resolution of the rain–gauge observations~~.

3.2.1 STREAP Calibration

The calibration process of STREAP using weather radar products was discussed in detail by Paschalis et al. (2013). Some modifications were made to tailor STREAP to the specific case study presented here. Due to the short period of the weather radar records (8 years), the storm arrival process (first module) was calibrated using the rain–gauge data (34 years). That allowed a better representation of the statistics of storm probability of occurrence and duration.

Changes were also applied to the second module. Originally, mean areal intensity and fraction of wet area during a storm are simulated as a bi-variate ~~autocorrelated~~ auto-correlated stochastic processes that also depend on storm duration. Here, due to the small extent of the spatial domain, the wet area ratio was assumed to be equal to zero during intra-storm periods and assumed to be equal to one during storms, i.e. during storms all grid cells over the catchment ~~were~~ are experiencing rainfall. The mean areal intensity is simulated using an AR(1) model which simulates a normalized quantile time series that is later inverted using a mixed-exponential function (Furrer and Katz, 2008; Smith and Schreiber, 1974), which parameters are computed using rain–gauge data.

No modifications were needed for the last module. However, some model parameters (e.g. rainfall coefficient of variation) could not be directly estimated from the weather radar data as the spatial resolution of the radar product (2 km) is too coarse compared to the model resolution (100 m). Therefore the required parameters were first estimated using the weather radar data for a coarse spatial resolution and then ~~scaled~~ downscaled to higher resolution using power law functions (Fig. S1 in the supplementary material) as described in ~~(Peleg et al., 2016) .~~ Peleg et al. (2016) . In addition, no direct measurements are available to estimate the small-scale rainfall spatial correlation structure for this region. The spatial structure was estimated using data from three dense rain-gauge networks (Moszkowicz, 2000; Müller and Haberlandt, 2016; Peleg et al., 2013) , recording rainfall over small spatial distances (i.e. in the scale of 10^1–10^2 m) and temporal scales (i.e. 5–10 min). The data is presented in Fig. S2.

3.2.2 STREAP Evaluation

The evaluation of STREAP, its ability to reproduce the rainfall intensity over the domain (with emphasis on the high rainfall intensity), and its performance with regard to the natural climate variability of the annual maxima in rainfall intensity, are discussed below.

The ability of STREAP to reproduce the rainfall intensity over the domain is shown using the inverse cumulative distribution function for the 10 min mean areal rainfall intensity (Fig. 3). Up to the 0.95 quantile, STREAP consistently underestimates the rainfall intensity, but this underestimation is minor (maximum difference 0.052 $mm\ h^{-1}$) and is not expected to bias the flow in the catchment. When we focus on the 0.95–1 quantile range which reflects the heavy rainfall intensity, and especially on the upper 0.99–1 quantile range, which represent the extremes, STREAP performs very well, with small differences between simulated and observed values (maximum difference 1.177 $mm\ h^{-1}$). The maximum difference and the maximum error cal-

culated for the 0.9995–1 quantile range, which covers ~~the entire~~ entirely annual maxima rainfall intensities that were observed, are as low as 1.072 $mm\ h^{-1}$ and 1.54 $\%$ (respectively). An example of STREAP ability to simulate spatially distributed annual maxima rainfall intensity over the catchment is given in Fig. 4. The ability of STREAP to reproduce the natural climate variability in relation to the annual maxima rainfall intensity is discussed and presented in the Supplementary Material (Fig. ~~S1~~S3).

3.3 Rainfall Cases Classification

Four rainfall cases were defined in order to account for climate variability and spatial rainfall variability and to allow the investigation of their effect on the urban drainage:

- Case 1: Consists of one time series of rainfall derived from the Lucerne rain–gauge (observed data, 34 years long). For this case, rainfall was not spatially distributed using STREAP but was uniformly distributed, i.e. same rainfall intensity was assigned to all sub-catchments for a given time step. In this case the rain–gauge time series represents also the mean areal rainfall over the catchment. ~~Thus~~ This is a common and critical assumption in hydrological studies, where point rainfall ~~represents~~ is used to represent areal rainfall (Rodriguez-Iturbe and Mejia, 1974; Peleg et al., 2016; Sivapalan and Bloschl, 1998; Svensson and Jones, 2010).

- Case 2: consists of 30 realizations of the same time series (rain–gauge observations) that was used in case 1, but spatially distributed using STREAP. Cases 1 and 2 differ in the spatial configuration of the rainfall (uniformly distributed vs. spatially distributed) which will later allow to explicitly analyze how the spatial rainfall variability ~~is affecting~~ affects the flow.

- Case 3: consists of 30 realizations of 30 years generated by STREAP. For this case, STREAP was set to generate only the mean areal rainfall and to uniformly distribute it over the sub-catchments (similar to case 1). Comparing the urban drainage response to the rainfall given from cases 1 and 3 will allow us to account for the climate variability component directly, as case 3 represents 30 alternative and equiprobable trajectories of the rainfall series given in case 1.

- Case 4: consists of 900 realizations accounting for both the spatial rainfall variability and the climate variability. Each of the 30 realizations ~~that were~~ generated for case 3 were re-generated 30 times using STREAP. The forcing has a different spatial distribution of the rainfall over the sub-catchments for each re-generation. This allows computing urban drainage dynamics subjected to the total variability.

3.4 Hydrodynamic Model

Flow simulations were conducted using USEPA's Storm Water Management Model (EPA SWMM), a dynamic 1-D model coupling rainfall–runoff processes with hydrodynamic channel flow (Rossman, 2010). EPA SWMM was chosen as it represents a standard open-source application in urban drainage modeling (e.g. Hsu et al., 2000; Liong et al., 1995; Meierdiercks et al., 2010).

EPA SWMM is composed of two modules: the surface runoff (hydrological) and the in-sewer flow (hydraulic) model. The hydrological model calculates the direct runoff under consideration of initial precipitation losses (i.e. evaporation and wetting losses) and soil infiltration (here using the Horton method). The resulting surface runoff is then used as input for the hydraulic model to simulate the pipe flow using the 1-D Saint-Venant equations. The diffusive wave approximation and a routing step of 10 s was applied for all simulations. Surface flooding is accounted for by allowing excess water to leave a manhole in case sewer capacity is exceeded. Due to the lack of detailed land use and surface topography data at meter scale it was found inadequate to further define a manhole-specific "ponding area" allowing the water to spread at the surface around a manhole. Hence excess water leaving the manhole is routed into a virtual sink and does not re-enter the system even though sewer capacity is available again.

The sewer model application is based on infrastructure data from the municipality's cadaster database. The model has carefully been calibrated and validated (split-sample approach) using the above mentioned one-year flow data record. Flow dynamics can be adequately reproduced throughout the year despite the rather coarse 10 min rainfall input data resolution. More details on the catchment, particularly on the urban land use characteristics, the monitoring set-up, model calibration procedure are given in Tokarczyk et al. (2015) . The runoff-generating surfaces are distributed over the entire catchment. This is represented by 158 individual sub-catchment entities with an area ranging between 0.02 and 0.84 ha. The rainfall fields generated by STREAP were intersected with the sub-catchment areas and rainfall intensity was assigned for each sub-catchment based on the weighted sum of the intersect area (cf. Gires et al., 2012). EPA SWMM was set-up for a continuous long-term simulation of 30 and 34 years, respectively, depending on the examined rainfall case. Unlike for the design-storm approach or the isolated analysis of single storm events as researched in many previous studies, antecedent hydrological conditions in the catchment and the drainage network are implicitly taken into account ~~here~~to fully address potential climatological changes also regarding dry spells.

3.5 Computation of IDF and FDF Curves

The ~~generalized extreme value~~ Generalized Extreme Value (GEV) distribution (Jenkinson, 1955) is commonly used in hydrological studies to model extreme rainfall intensity (e.g. Koutsoyiannis and Baloutsos, 2000; Marra and Morin, 2015) and flows (e.g Zaidman et al., 2003) since it covers the Gumbel, Fréchet and Weibull distributions (Katz et al., 2005). IDF and FDF curves were calculated by fitting a GEV distribution to the series of annual maxima of the mean areal rainfall intensity and the conduit flow time series (respectively). The fitting of the parametric distribution is a required step for the partition analysis to be conducted (see next section) as it results in a continuous estimates of the curves quantiles (i.e. the return period).

IDF curves were calculated for two datasets: observed data derived from the Lucerne rain–gauge and simulated data that were generated using STREAP. For the observed dataset, one IDF curve was computed for the 34 years of records. For the simulated dataset, 30 IDF curves were calculated for the 30 stochastic realizations (of 30 years each). The curves were calculated for a 10 min duration.

FDF curves were calculated for the simulated flow at three locations which were chosen according to their function within the drainage network (see Fig. 1): (i) about 200 m upstream of the combined sewer overflows (CSO) structure in a sewer section

that was previously identified as prone to pipe surcharge (location A - inner network node); (ii) about 200 m downstream of the CSO structure (location B – carry-on flow to sewage treatment works); and (iii) at the CSO outlet to lake (location C - overflow). The number of derived FDF curves follow the rainfall cases as described in Section 3.3, i.e. 1 for the first case (34 years), 30 for the second and third cases (30 years each) and 900 for the fourth case (30 years each). FDF curves were calculated for a 5 min duration.

Note that no condition was imposed on the time concurrency of annual maxima of mean areal rainfall intensity and conduit flow, i.e. annual peak flow can precede, overlap or follow the annual maxima of mean areal rainfall intensity.

3.6 Variability Partitioning

The partition method used in this study follows the guidelines suggested by Fatichi et al. (2016). We assume that there are interactions between the two sources of variability~~(~~, i.e. they cannot be treated independently~~)~~ , as the spatial pattern of the rainfall annual maxima is dependent on the extreme rainfall intensity that is driven by a given climate trajectory. The climate variability, CLM, is defined as the 5–95 quantile range of the flow that is calculated using the 30 spatial uniform climate realizations simulated for case 3 (i.e. the outcome is one flow range for a given return period). ~~The~~ For each of the 30 climate realizations, the spatial rainfall variability, SPT, is defined as the 5–95 quantile difference of the flow calculated ~~for each of the 30 climate realizations using the 30 spatially variable realizations~~ using the spatially variable rainfall simulated for case ~~4 (i.e. the~~ 4. The outcome is 30 different flow ranges, $SPT^1_{RP}, SPT^2_{RP}, ..., SPT^{30}_{RP}$, one for each climate trajectory and for a given return period~~)~~. The 5–95 quantile range was used because of the different sample sizes between case 3 (30 realizations) and case 4 (900 realizations). The ~~contribution of~~ ratio between the climate variability, ~~φ_{CLM} to~~ CLM and the total variability, TOT, for each return period, RP, can then be estimated as:

$$\varphi_{CLM,RP} = \frac{CLM_{RP}}{TOT_{RP}} \tag{1}$$

where the total variability for a given return period is the difference between the maximum and minimum spatial variability simulated per return period from all climate trajectories:

$$TOT_{RP} = \max SPT_{RP} - \min SPT_{RP} \tag{2}$$

~~Note that the~~ The total variability for a given return period, TOT_{RP} , ~~calculated above~~ will be always smaller ~~comparing to the total variability that will be calculated by summing~~ than the sum of the flow variability from case 4, because there is a dependency between the two sources of uncertainty. Note that $1-\varphi_{CLM,RP}$ is representing the unique contribution of spatial variability to the total variability for a given return period, however the total spatial variability, $\frac{\sum_{i=1}^{N} SPT^i_{RP}}{N}$, is larger or equal to $1-\varphi_{CLM,RP}$ (see Fatichi et al., 2016) . An illustrative example for the partition method is given in Fig. 5.

4 Results and Discussion

In the following, we present computed IDF (rain) and FDF (flow) curves and discuss the contributions of individual rainfall variabilities to the modelled sewage flow variability at three different locations: A – inner network node (Fig. ~~S2 and~~ S4 and

S6), B - carry-on flow (Fig. 6 and 7), and C - combined sewer overflow (Fig. ~~S3 and~~ S5 and S7). The partitioning of the flow variability ~~was conducted~~ is presented for all three locations (Fig. 8).

The effect of spatial rainfall variability on the flow can be directly estimated by examining the flow variability from case 2 (Fig. 6c, S2c and S4c). The effect of spatial rainfall variability is derived from the analysis of flow extremes occurring in a continuous time series of 30 years. The variability in annual flow maxima is computed from the spread in simulations for a given return period. This variability is expressed here in its simplest form, as the difference between the highest and lowest flows simulated for the 30 realizations for a given return period. The effect of spatial rainfall variability on urban hydrology was researched in the past (e.g. Bruni et al., 2015; Gires et al., 2012; Simoes et al., 2015; Willems and Berlamont, 2002) leading to the conclusion that this variability should be taken into consideration when running urban hydrological models. Indeed, for return periods between 2 and 30 years, the peak flow variability was found to vary between 18.3 and 55.1 $l\ s^{-1}$ at location A (Fig. ~~S2c) and~~ S4c) and between 91.2 and 179 $l\ s^{-1}$ at location C (Fig. ~~S4c~~S6c). At location B, peak flow variability was found to be ~~low (vary~~ lower (between 2.9 and 6.2 $l\ s^{-1}$, Fig. 6c) due to the fact that flow is hydraulically constrained ~~though~~ by the upstream located throttle pipe.

The effect of the climate variability over the catchment is calculated from the 30 rainfall realizations stochastically simulated for cases 3 and 4 (left panel in Fig. 7). Similar to the flow variability, the climate variability is expressed as the difference between the highest and lowest mean areal rainfall found for a given return period. In agreement with Peleg et al. (2016), the climate variability was found to increase with longer return periods, from 11.8 $mm\ h^{-1}$ for the two year return period to 47.2 $mm\ h^{-1}$ for the 30 year return period.

The effect of the climate variability on the flows in the catchment is estimated from case 3 (Fig. 7b, S3b and S5b). For the return periods of 2 to 30 years, the flow variability at location C, resulting only from climate variability, was found to be in the range 278.9–420.3 $l\ s^{-1}$. For most of the return periods this variability ~~is~~ more than doubles the flow variability resulting from the spatial rainfall variability. The results for location C suggest that the role of climate variability is considerably more important than the role of spatial rainfall variability. The flow variability for the return periods 2–30 years for locations A and B were found to be in the range of 33.3–48.5 and 7.3–11.6 $l\ s^{-1}$ (respectively). As for location C, the flow variability resulting from climate variability is higher than the flow variability resulting from the spatial rainfall variability. However, the relative differences in variability around the median peak flow, calculated for the 30 years return period, reveal that the differences between the individual variabilities are much less ~~meaningful~~ pronounced for locations A and B (1.7% to 3.2% and 0.8% to 2.1%, respectively) in comparison to location C (3.5% to 10.7%). ~~The~~ These differences regarding the absolute flow variability are expected as location B is located downstream of a hydraulic constraint (throttle pipe at CSO structure), thus flow is eventually levelled out, while at location A runoff is drained directly from its ~~associated~~ contributing sub-catchment without any buffering but still constrained due to surface flooding, i.e. excess flows leave the manhole through the lid and do not contribute to the actual peak flow.

The total flow variability is calculated using the data of case 4 (Fig. 7c). As expected, the total flow variability is larger than the flow variability resulting from either the spatial rainfall variability (case 2, Fig. 6) or from the climate variability alone (case 3, Fig. 7). The partitioning of the total flow variability into its ~~individual sources~~ components is presented for all three

locations in Fig. 8. Results indicate that climate variability is the dominant contributor of the total variability of flow in the catchment. This applies to peak flows analyzed at all three locations in the urban drainage system. The highest ~~contribution of the climate variability to~~ ratio between climate variability and total variability is for location B, 83% for 2.2 years return period, and decreases for longer return periods to 57% for the 30 years return period. This decreasing trend was found to be less prominent for locations A and C, but statistically significant for all three locations as supported by a trend analysis using the Mann-Kendall test (Kendall, 1975; Mann, 1945). For location A, the relative mean ~~contribution of the climate~~ ratio between the climate and the total variability was found to be around 81%. For location C, ~~the mean contribution of climate variability was found to be~~ climate variability accounts for 75% for the 2 to 10 year return periods, decreasing to 62% for the 30 year return period. Averaged over all three locations and all return periods the mean ~~contribution of~~ ratio between the climate variability ~~to~~ and the total variability is 74%, leaving 26% contribution ~~from~~ due to the addition of spatial variability. The results of the partitioning suggests that using traditional methods to quantify variability in urban drainage, such as bootstrapping, will likely result in an underestimation of the variability (and uncertainty) as only the climate variability will be represented. This is especially important for return periods that are longer than 10 years. While the use of spatially distributed rainfall data can supply valuable information for sewer network design (based on rainfall with return periods from 5 to 15 years), it will become even more important when performing flood risk assessments of extreme events (larger return periods).

The rainfall generator was used to simulate rainfall for the weather radar subpixel scale, i.e. in a finer spatial resolution than can be estimated using the MeteoSwiss radar. The rainfall data required for a complete validation of the rainfall generator for this resolution can be obtained from a dense rain–gauge network (for networks examples see Muthusamy et al., 2016; Peleg et al., 2013) but such a network is not available ~~for our~~ in the analyzed region. Therefore some assumptions ~~need to be~~ were made. Two of those assumptions ~~should be~~ are discussed in the light of missing information for the subpixel scale: (i) the rain fields are simulated following a lognormal distribution. We assume that the non-zero part of the subpixel spatial rainfall distribution follows the observed lognormal distribution that is recorded by the weather radar for this region (as in Paschalis et al., 2014; Peleg et al., 2016). ~~Choosing a~~ A different spatial rainfall distribution ~~to follow~~ will significantly affects the results of the extreme rainfall distribution; (ii) we assume that ~~same~~ occurrence and intensity statistics are ~~applied~~ equal for each of the grid cells~~equally~~, i.e. no ~~filter~~ spatial correlation is applied for the ~~spatial~~ rainfall occurrence or intensity. That means that ~~no~~ orographic, distance from the lake or urban micro-climate effects are ~~considered. Provided they are known these effects can be included.~~ not considered. No automatic calibration process exists for STREAP. The model requires not only high-resolution rainfall data but also an expert user for the calibration process, as modifications ~~for~~ to the calibration procedure (e.g. ~~for this study, scaling for~~ scaling at higher spatial resolution) are needed in order to tailor STREAP ~~for a given location.~~ to a given application.

The three locations analyzed in this study were deliberately chosen according to their functional hierarchy within the combined drainage system (i.e. inner network node, carry-on flow and overflow). By doing so, we can clearly differentiate the effect of spatial and climatological rainfall variability on elements depending on their function within the network. On the other hand, previous studies showed a tendency that conduits located upstream, not affected by hydraulically constraining structures, are more sensitive to rainfall spatial variability in comparison to conduits located downstream (e.g. Gires et al., 2012) . While

it would be interesting to further investigate flow variability due to different spatial rainfall characteristics (e.g. the rainfall spatial correlation) at various upstream locations (similar as location A), this type of analysis would require larger drainage networks in comparison to the one presented here. Future studies will benefit from examining several different urban drainage systems with rainfall input from different high-resolution products to test the robustness of the findings.

The computational cost of running a rainfall generator combined with an urban drainage model ~~is also a matter for discussion~~may constrain the use of the proposed approach for practical applications. But given the advances in the availability of computing capacity, also for non-scientific institutions, such application will becomes feasible in the near future. We have used a powerful 20 core desktop machine (Intel Xeon CPU E5-2687W) to run the 961 stochastic rainfall realizations with STREAP in approximately 4 days. We estimated that the time needed to run SWMM using the same ~~machine will be~~ stand-alone machine would have been about 4 months~~. This is a too prolong time~~, which is impractically long duration, especially considering the small size of the urban catchment. ~~Ultimately~~Therefore, we have used ~~an HPCcluster, a collection of~~ a high performance computing (HPC) cluster with hundreds of computing nodes allowing ~~high-performance scientific computations, to run~~ SWMM simulations in less than 48 hours.

5 Conclusions

Output from a stochastic rainfall generator was used as ~~an~~ input into an urban drainage model to investigate the effect of spatial rainfall variability and climate variability on peak flows in an urban drainage system located in central Switzerland. ~~It is~~ We found that the climate variability is the main contributor (74 % on average) to the total flow variability, but that the relative contribution of the addition of spatial rainfall variability increases with return period.

The analysis presented in this study was conducted at three different locations in the urban drainage system which reflect different system functions. Deviations in flow quantities and dynamics were expected and are, in fact, observed within the catchment depending on the corresponding location (i.e. up- or downstream of the overflow structure, or the overflow itself). Despite this, in agreement for all three locations we found that the climate variability is the ~~dominate~~ dominant contributor to the flow variability for all return periods.

We present ~~only~~ a single case study, a relatively small, but typical urban catchment located in the foothills of the Swiss Alps. However, we argue that the ~~partitioning of the spatial rainfall variability and climate variability~~ variability partitioning is likely to be similar for most ~~small to medium size urban catchment, meaning that~~ small– to medium–sized urban catchments. That is to say, the climate variability will constitute the largest contribution to the overall flow variability also in other urban catchments, and spatial variability will gain more importance as longer return periods are being considered. ~~It is probable that the contribution of~~ Further investigations are needed to examine the contributions of the variability components in larger catchments (potentially more prone to spatial rainfall variability~~will increase with increasing of the urban catchment area, however a further investigation is needed to establish this as it can be buffered by the complexity of the drainage system, e.g. by compensating due to hydraulic inner network dependencies~~) with a more complex drainage network (potentially with more flow attenuation).

Regarding the added value in using high resolution stochastic rainfall generators for urban drainage applications, ~~based on our results~~ we conclude that not addressing the spatial rainfall variability will result in a ~~significant~~ considerable underestimation of the ~~variability~~ uncertainty in catchment response, especially for longer return periods which are likely of main interest. Stochastic rainfall generators should become an integral part of the urban hydrologist toolbox, particularly when estimating hazards of urban flooding. However, these methods are still not commonly used by planning engineers for designing and evaluating urban drainage systems. We identify ~~three~~ four main aspects that contribute to the reluctant acceptance among practitioners:

- High-resolution rainfall data are required (from a weather radar system or from a dense rain–gauge network) as well as an expert user for the calibration process. Setting up an automatic calibration process is ~~however not a realistic~~ unrealistic option due to the spatio-temporal differences between weather radar systems and the need to tailor the rainfall generator ~~for~~ to specific locations.

- The high computational cost of running a rainfall generator combined with an urban drainage model may be prohibitive for common applications~~, even for a small urban catchment. The resources requires~~ . Today the resources required for an efficient ~~time-consuming~~ computation (e.g. HPC cluster) are often not (yet) available in the private sector.

- The struggle to overcome old engineering paradigms towards accepting variability ranges as useful information ~~on the one hand and the~~ for design and performance assessment.

- The difficulty of rainfall generators modelers to transparently convey the modeling chain, its results and uncertainties~~on the other hand~~.

These aspects should be addressed in future ~~development~~ applications of high-resolution stochastic rainfall generators in order to make them more accessible to the urban drainage community.

Acknowledgements. This project is partly funded by the Swiss Competence Center for Energy Research – Supply of Electricity. We are grateful to MeteoSwiss, the Swiss Federal Office of Meteorology and Climatology, and the city of Lucerne for providing us with precipitation and infrastructure data. We furthermore would like to thank the Engineering Consultants from HOLINGER AG, Bern for assisting us with details on the hydraulic model and extracting operation data from the central data base. We thank the reviewers (Susana Ochoa-Rodriguez, Li-Pen Wang and an anonymous reviewer) and to Marie-Claire ten Veldhuis, the editor, for their contributions leading to a significantly increased quality of the paper.

References

Berne, A., Delrieu, G., Creutin, J.-D., and Obled, C.: Temporal and spatial resolution of rainfall measurements required for urban hydrology, Journal of Hydrology, 299, 166 – 179, doi:http://dx.doi.org/10.1016/j.jhydrol.2004.08.002, 2004.

Bruni, G., Reinoso, R., van de Giesen, N. C., Clemens, F. H. L. R., and ten Veldhuis, J. A. E.: On the sensitivity of urban hydrodynamic modelling to rainfall spatial and temporal resolution, Hydrology and Earth System Sciences, 19, 691–709, doi:10.5194/hess-19-691-2015, 2015.

Deser, C., Knutti, R., Solomon, S., and Phillips, A. S.: Communication of the role of natural variability in future North American climate, Nature Climate Change, 2, 775–779, doi:10.1038/nclimate1562, 2012.

Fatichi, S., Ivanov, V. Y., Paschalis, A., Peleg, N., Molnar, P., Rimkus, S., Kim, J., Burlando, P., and Caporali, E.: Uncertainty partition challenges the predictability of vital details of climate change, Earth's Future, 4, 240–251, doi:10.1002/2015EF000336, 2016.

Foresti, L., Reyniers, M., Seed, A., and Delobbe, L.: Development and verification of a real-time stochastic precipitation nowcasting system for urban hydrology in Belgium, Hydrology and Earth System Sciences, 20, 505–527, doi:10.5194/hess-20-505-2016, 2016.

Furrer, E. M. and Katz, R. W.: Improving the simulation of extreme precipitation events by stochastic weather generators, Water Resources Research, 44, n/a–n/a, doi:10.1029/2008WR007316, 2008.

Gabella, M., Bolliger, M., Germann, U., and Perona, G.: Large sample evaluation of cumulative rainfall amounts in the Alps using a network of three radars, Atmospheric Research, 77, 256 – 268, doi:http://dx.doi.org/10.1016/j.atmosres.2004.10.014, 2005.

Germann, U., Galli, G., Boscacci, M., and Bolliger, M.: Radar precipitation measurement in a mountainous region, Quarterly Journal of the Royal Meteorological Society, 132, 1669–1692, doi:10.1256/qj.05.190, 2006.

Germann, U., Boscacci, M., Gabella, M., and Sartori, M.: Radar design for prediction in the Swiss Alps, Meteorol. Technol. Int, 4, 42–45, 2015.

Gires, A., Onof, C., Maksimovic, C., Schertzer, D., Tchiguirinskaia, I., and Simoes, N.: Quantifying the impact of small scale unmeasured rainfall variability on urban runoff through multifractal downscaling: A case study, Journal of Hydrology, 442–443, 117 – 128, doi:http://dx.doi.org/10.1016/j.jhydrol.2012.04.005, 2012.

Gires, A., Tchiguirinskaia, I., Schertzer, D., and Lovejoy, S.: Multifractal analysis of a semi-distributed urban hydrological model, Urban Water Journal, 10, 195–208, doi:10.1080/1573062X.2012.716447, 2013.

Guo, Y.: Updating Rainfall IDF Relationships to Maintain Urban Drainage Design Standards, Journal of Hydrologic Engineering, 11, 506–509, doi:10.1061/(ASCE)1084-0699(2006)11:5(506), 2006.

Hawkins, E. and Sutton, R.: The Potential to Narrow Uncertainty in Regional Climate Predictions, Bulletin of the American Meteorological Society, 90, 1095–1107, doi:10.1175/2009BAMS2607.1, 2009.

Hsu, M., Chen, S., and Chang, T.: Inundation simulation for urban drainage basin with storm sewer system, Journal of Hydrology, 234, 21 – 37, doi:http://dx.doi.org/10.1016/S0022-1694(00)00237-7, 2000.

Jenkinson, A. F.: The frequency distribution of the annual maximum (or minimum) values of meteorological elements, Quarterly Journal of the Royal Meteorological Society, 81, 158–171, doi:10.1002/qj.49708134804, 1955.

Katz, R. W., Brush, G. S., and Parlange, M. B.: STATISTICS OF EXTREMES: MODELING ECOLOGICAL DISTURBANCES, Ecology, 86, 1124–1134, doi:10.1890/04-0606, 2005.

Kendall, M. G.: Rank correlation methods., 1975.

Koutsoyiannis, D. and Baloutsos, G.: Analysis of a Long Record of Annual Maximum Rainfall in Athens, Greece, and Design Rainfall Inferences, Natural Hazards, 22, 29–48, doi:10.1023/A:1008001312219, 2000.

Koutsoyiannis, D., Kozonis, D., and Manetas, A.: A mathematical framework for studying rainfall intensity-duration-frequency relationships, Journal of Hydrology, 206, 118 – 135, doi:http://dx.doi.org/10.1016/S0022-1694(98)00097-3, 1998.

Liong, S.-Y., Chan, W. T., and ShreeRam, J.: Peak-Flow Forecasting with Genetic Algorithm and SWMM, Journal of Hydraulic Engineering, 121, 613–617, doi:10.1061/(ASCE)0733-9429(1995)121:8(613), 1995.

Mann, H. B.: Nonparametric tests against trend, Econometrica: Journal of the Econometric Society, pp. 245–259, 1945.

Marra, F. and Morin, E.: Use of radar {QPE} for the derivation of Intensity–Duration–Frequency curves in a range of climatic regimes, Journal of Hydrology, 531, Part 2, 427 – 440, doi:http://dx.doi.org/10.1016/j.jhydrol.2015.08.064, 2015.

McRobie, F. H., Wang, L.-P., Onof, C., and Kenney, S.: A spatial-temporal rainfall generator for urban drainage design, Water Science and Technology, 68, 240–249, doi:10.2166/wst.2013.241, 2013.

Meierdiercks, K. L., Smith, J. A., Baeck, M. L., and Miller, A. J.: Analyses of Urban Drainage Network Structure and its Impact on Hydrologic Response1, JAWRA Journal of the American Water Resources Association, 46, 932–943, doi:10.1111/j.1752-1688.2010.00465.x, 2010.

Müller, H. and Haberlandt, U.: Temporal rainfall disaggregation using a multiplicative cascade model for spatial application in urban hydrology, Journal of Hydrology, pp. –, doi:http://dx.doi.org/10.1016/j.jhydrol.2016.01.031, 2016.

Moszkowicz, S.: Small-scale structure of rain field — Preliminary results basing on a digital gauge network and on MRL-5 legionowo radar, Physics and Chemistry of the Earth, Part B: Hydrology, Oceans and Atmosphere, 25, 933 – 938, doi:http://dx.doi.org/10.1016/S1464-1909(00)00128-3, 2000.

Muthusamy, M., Schellart, A., Tait, S., and B. M. Heuvelink, G.: Geostatistical upscaling of rain gauge data to support uncertainty analysis of lumped urban hydrological models, Hydrology and Earth System Sciences Discussions, 2016, 1–27, doi:10.5194/hess-2016-279, 2016.

Niemi, T. J., Guillaume, J. H. A., Kokkonen, T., Hoang, T. M. T., and Seed, A. W.: Role of spatial anisotropy in design storm generation: Experiment and interpretation, Water Resources Research, 52, 69–89, doi:10.1002/2015WR017521, http://dx.doi.org/10.1002/2015WR017521, 2016.

Ochoa-Rodriguez, S., Wang, L.-P., Gires, A., Pina, R. D., Reinoso-Rondinel, R., Bruni, G., Ichiba, A., Gaitan, S., Cristiano, E., van Assel, J., Kroll, S., Murla-Tuyls, D., Tisserand, B., Schertzer, D., Tchiguirinskaia, I., Onof, C., Willems, P., and ten Veldhuis, M.-C.: Impact of spatial and temporal resolution of rainfall inputs on urban hydrodynamic modelling outputs: A multi-catchment investigation, JOURNAL OF HYDROLOGY, 531, 389–407, doi:10.1016/j.jhydrol.2015.05.035, 2015.

Panziera, L., Gabella, M., Zanini, S., Hering, A., Germann, U., and Berne, A.: A radar-based regional extreme rainfall analysis to derive the thresholds for a novel automatic alert system in Switzerland, Hydrology and Earth System Sciences, 20, 2317–2332, doi:10.5194/hess-20-2317-2016, 2016.

Paschalis, A., Molnar, P., Fatichi, S., and Burlando, P.: A stochastic model for high-resolution space-time precipitation simulation, Water Resources Research, 49, 8400–8417, doi:10.1002/2013WR014437, http://dx.doi.org/10.1002/2013WR014437, 2013.

Paschalis, A., Fatichi, S., Molnar, P., Rimkus, S., and Burlando, P.: On the effects of small scale space–time variability of rainfall on basin flood response, Journal of Hydrology, 514, 313 – 327, doi:http://dx.doi.org/10.1016/j.jhydrol.2014.04.014, 2014.

Peleg, N. and Morin, E.: Stochastic convective rain-field simulation using a high-resolution synoptically conditioned weather generator (HiReS-WG), Water Resources Research, 50, 2124–2139, doi:10.1002/2013WR014836, http://dx.doi.org/10.1002/2013WR014836, 2014.

Peleg, N., Ben-Asher, M., and Morin, E.: Radar subpixel-scale rainfall variability and uncertainty: lessons learned from observations of a dense rain-gauge network, Hydrology and Earth System Sciences, 17, 2195–2208, doi:10.5194/hess-17-2195-2013, 2013.

Peleg, N., Shamir, E., Georgakakos, K. P., and Morin, E.: A framework for assessing hydrological regime sensitivity to climate change in a convective rainfall environment: a case study of two medium-sized eastern Mediterranean catchments, Israel, Hydrology and Earth System Sciences, 19, 567–581, doi:10.5194/hess-19-567-2015, 2015.

Peleg, N., Marra, F., Fatichi, S., Paschalis, A., Molnar, P., and Burlando, P.: Spatial variability of extreme rainfall at radar subpixel scale, Journal of Hydrology, doi:doi:10.1016/j.jhydrol.2016.05.033, 2016.

Rodriguez-Iturbe, I. and Mejia, J. M.: On the transformation of point rainfall to areal rainfall, Water Resources Research, 10, 729–735, doi:10.1029/WR010i004p00729, 1974.

Rossman, L. A.: Storm water management model user's manual, version 5.0, National Risk Management Research Laboratory, Office of Research and Development, US Environmental Protection Agency Cincinnati, OH, 2010.

Sideris, I. V., Gabella, M., Erdin, R., and Germann, U.: Real-time radar–rain-gauge merging using spatio-temporal co-kriging with external drift in the alpine terrain of Switzerland, Quarterly Journal of the Royal Meteorological Society, 140, 1097–1111, doi:10.1002/qj.2188, 2014.

Simoes, N. E., Ochoa-Rodriguez, S., Wang, L.-P., Pina, R. D., Marques, A. S., Onof, C., and Leitao, J. P.: Stochastic Urban Pluvial Flood Hazard Maps Based upon a Spatial-Temporal Rainfall Generator, Water, 7, 3396, doi:10.3390/w7073396, 2015.

Sivapalan, M. and Bloschl, G.: Transformation of point rainfall to areal rainfall: Intensity-duration-frequency curves, Journal of Hydrology, 204, 150 – 167, doi:http://dx.doi.org/10.1016/S0022-1694(97)00117-0, 1998.

Smith, R. E. and Schreiber, H. A.: Point processes of seasonal thunderstorm rainfall: 2. Rainfall depth probabilities, Water Resources Research, 10, 418–423, doi:10.1029/WR010i003p00418, 1974.

Svensson, C. and Jones, D.: Review of methods for deriving areal reduction factors, Journal of Flood Risk Management, 3, 232–245, doi:10.1111/j.1753-318X.2010.01075.x, 2010.

Tokarczyk, P., Leitao, J. P., Rieckermann, J., Schindler, K., and Blumensaat, F.: High-quality observation of surface imperviousness for urban runoff modelling using UAV imagery, Hydrology and Earth System Sciences, 19, 4215–4228, doi:10.5194/hess-19-4215-2015, http://www.hydrol-earth-syst-sci.net/19/4215/2015/, 2015.

Vaes, G., Willems, P., and Berlamont, J.: Rainfall input requirements for hydrological calculations, Urban Water, 3, 107 – 112, doi:http://dx.doi.org/10.1016/S1462-0758(01)00020-6, 2001.

Willems, P.: A spatial rainfall generator for small spatial scales, Journal of Hydrology, 252, 126 – 144, doi:http://dx.doi.org/10.1016/S0022-1694(01)00446-2, 2001.

Willems, P. and Berlamont, J.: Accounting for the spatial rainfall variability in urban modelling applications, Water Science and Technology, 45, 105–112, 2002.

Wright, D. B., Smith, J. A., and Baeck, M. L.: Flood frequency analysis using radar rainfall fields and stochastic storm transposition, Water Resources Research, 50, 1592–1615, doi:10.1002/2013WR014224, 2014a.

Wright, D. B., Smith, J. A., Villarini, G., and Baeck, M. L.: Long-Term High-Resolution Radar Rainfall Fields for Urban Hydrology, JAWRA Journal of the American Water Resources Association, 50, 713–734, doi:10.1111/jawr.12139, 2014b.

Yazdanfar, Z. and Sharma, A.: Urban drainage system planning and design – challenges with climate change and urbanization: a review, Water Science and Technology, 72, 165–179, doi:10.2166/wst.2015.207, 2015.

Zaidman, M. D., Keller, V., Young, A. R., and Cadman, D.: Flow-duration-frequency behaviour of British rivers based on annual minima data, Journal of Hydrology, 277, 195 – 213, doi:http://dx.doi.org/10.1016/S0022-1694(03)00089-1, 2003.

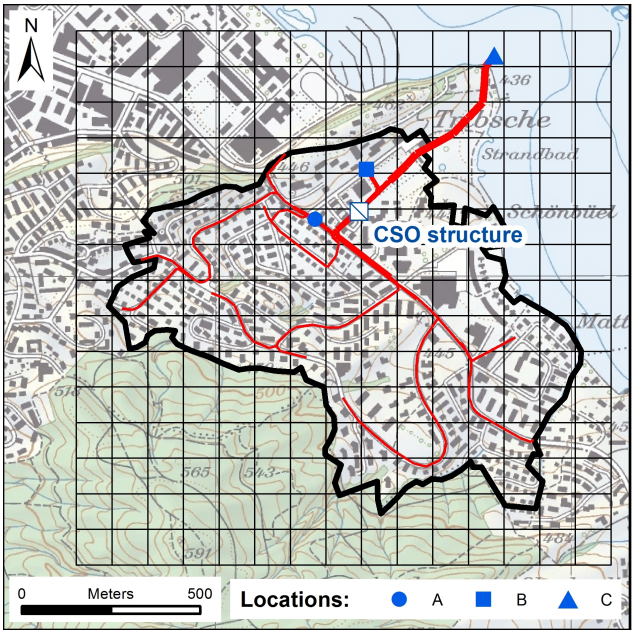

Figure 1. Location map of the case study catchment (bounded with black line). The black mesh represents the 1.5 x 1.5 km^2 domain (grid cell resolution of 100 x 100 m^2) for which stochastic rainfall was generated. The red lines represent the drainage system (thicker lines per pipe diameter) and the blue circle (inner network node), rectangle (carry-on flow) and triangle (combined sewer overflow) symbols represent the location for which the flow analysis was conducted. The combined sewer overflows (CSO structure~~(~~, blue romb symbol) is located between locations A and B.

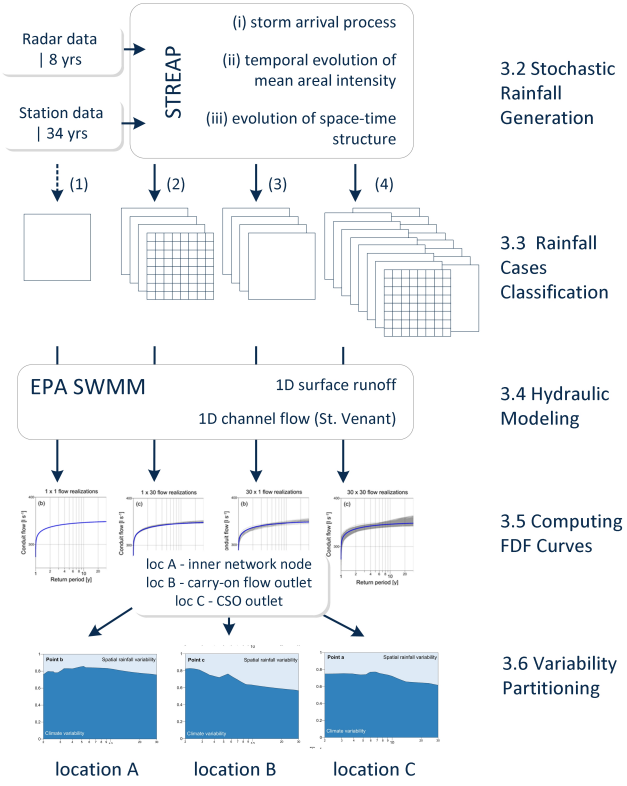

Figure 2. A schematic illustration of the methods used in this study: (i) STREAP model was used to simulate multiple realizations of 2-D rain fields based on radar and gauged data (Section 3.2); (ii) rainfall was generated for four distinct cases which were defined in order to explicitly account for the climate variability, spatial rainfall variability and total variability of the flow (3.3); (iii) EPA SWMM model was used to calculate the flow over the catchment (3.4); (iv) IDF and FDF curves were computed for the annual maxima of the mean areal rainfall and flow, respectively, at three different locations (3.5); and (v) the total flow variability was partitioned (3.6).

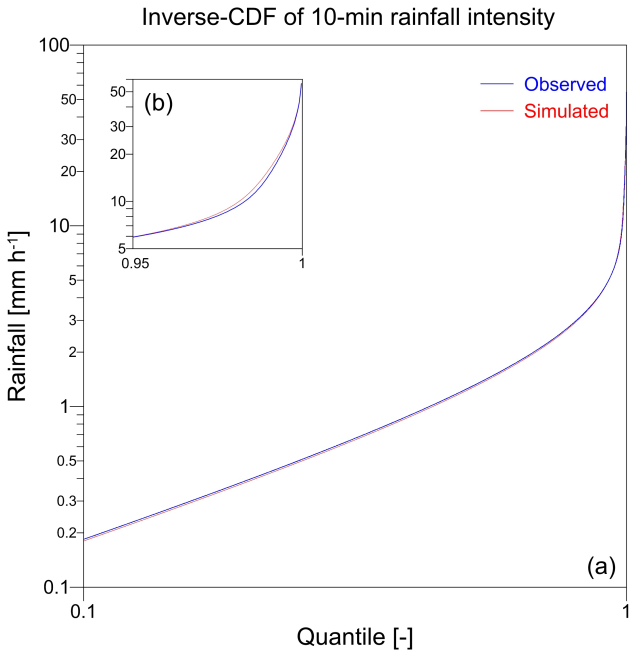

Figure 3. An inverse cumulative distribution function of the 10 min mean areal rain intensity over the catchment [The 0.1–1 quantile is presented in (a) and the 0.95–1 quantile range is zoomed in (b)]. Blue line represents 34 years of observed data (1981–2014) and red line represents the median of 30 realizations of 30 years. The simulated mean 5–95 quantile range of the rainfall intensity of the 30 realizations is also presented (shaded red).

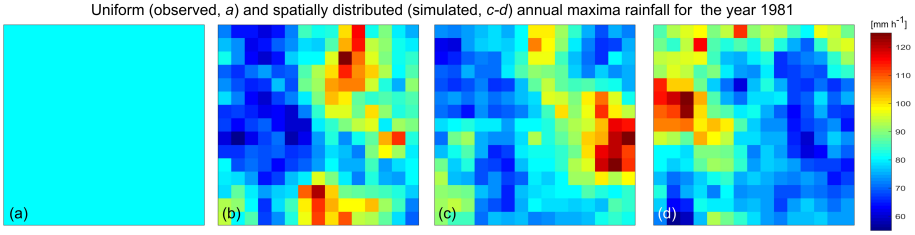

Figure 4. An example of STREAP ability to spatially distribute the annual maxima rainfall intensity over the catchment. The annual maxima recorded by Lucerne gauge for the year 1981 is 80.4 $mm\ h^{-1}$ for duration of 10 min. Without STREAP, this value is assumed to be uniformly distributed over the domain (panel a). STREAP accounts for the spatial distribution of rainfall, thus while the areal average is preserved for each time step, some grid cells (100 x 100 m^2 resolution) will record higher rainfall intensity and some lower values. Example of the footprint of the annual maxima rainfall intensity for three random realizations of the year 1981 generated by STREAP are presented in panels b–d.

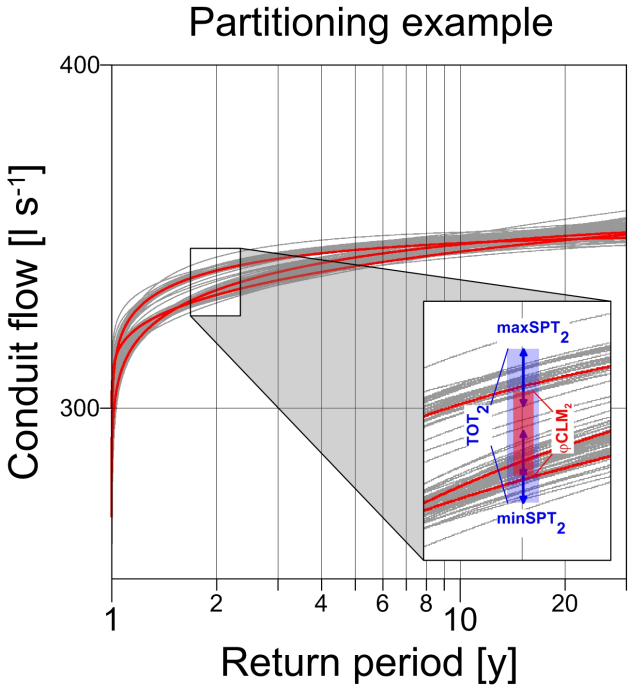

Figure 5. An example for the partition method (illustrative) for the 2 years return period (zoomed panel). 3 climate trajectories are plotted (red lines) for which the 5–95 quantile range is calculated ($\varphi_{CLM,2}$, red area). For each climate trajectory, 30 spatial realizations are plotted (grey lines). The 5–95 quantile range is ~~than~~ then calculated for each of the 30 spatial realizations ($SPT_2^1, SPT_2^2, SPT_2^3$, plotted as blue arrows) and the total variability, TOT_2 (blue area), is defined by bounding the maximum and minimum flows defined by the spatial variability ($\max SPT_2$ and $\min SPT_2$, respectively). The partition of the climate variability, $\varphi_{CLM,2}$, out of the total variability is then calculated as a simple ~~division~~ ratio between the two.

.

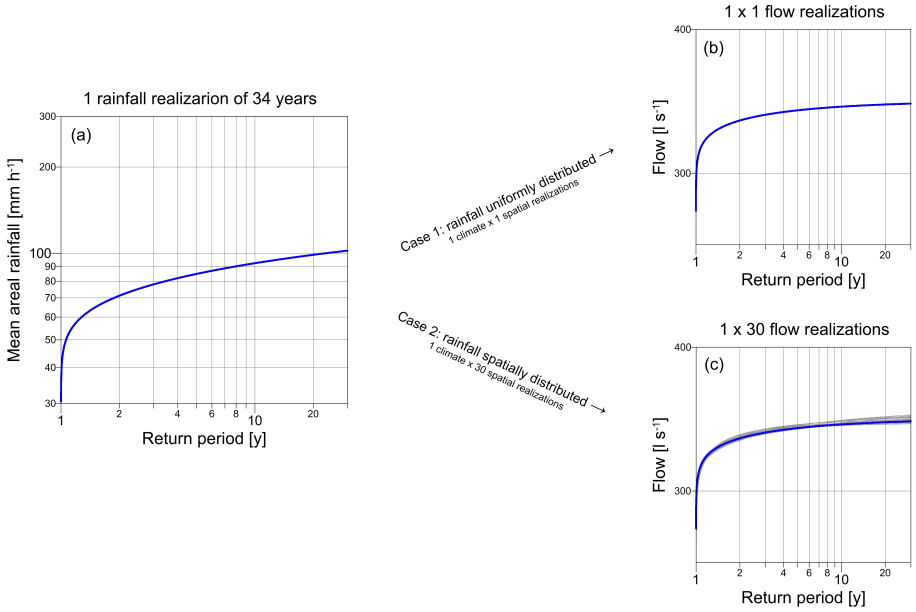

Figure 6. Rainfall and flow results for cases 1 and 2. In the left panel, the IDF curve computed for the mean areal rainfall over the catchment is presented. In the right panels, FDF curves for location B are presented. Blue line represents the IDF curve and the FDF curves computed from the observed uniformly distributed rainfall. Gray lines represent the FDF curves computed for the realizations with spatial rainfall variability.

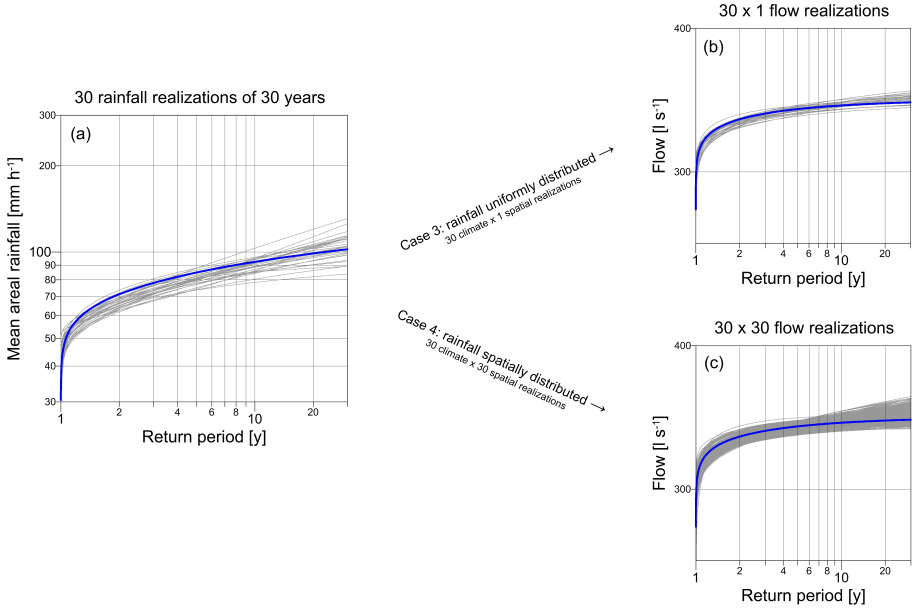

Figure 7. Same as Fig. 6, but for cases 3 and 4.

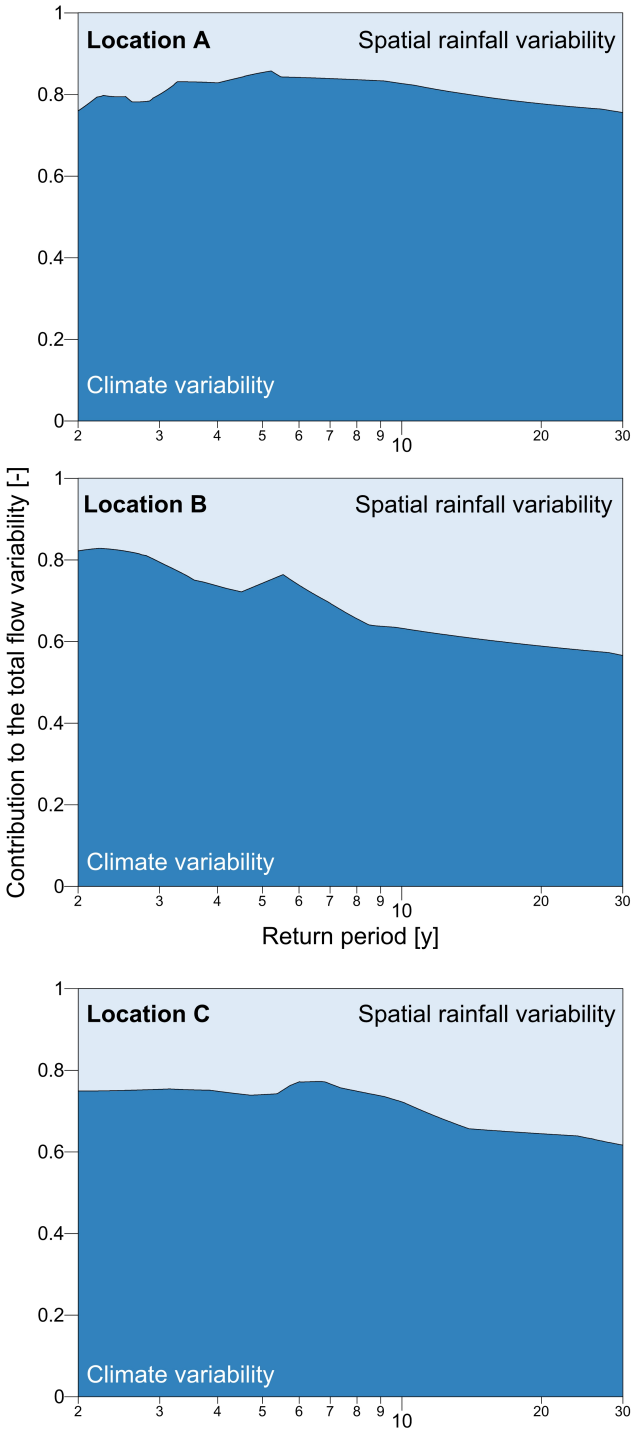

Figure 8. The ~~contribution of~~ ratio between the ~~spatial rainfall variability (light blue area) and~~ climate variability ~~(dark blue area) to~~ and the total flow variability for a given return period and for different locations within the urban drainage system is represented in dark blue. The remaining contribution is due to the addition of spatial rainfall variability (light blue).